Mechanistic Aspects of F^+ Transfer Reactions: A Model Study in the Gas Phase

Massimiliano Aschi,* Felice Grandinetti,* and Vittorio Vinciguerra

Abstract: The mechanism of the spin-forbidden formal F^+ transfer from $^1NF_2^+$ to CO with formation of $^1FCO^+$ and ^3NF was investigated by mass spectrometry and high-level theoretical calculations. The $(NF_2CO)^+$ intermediates involved in this process, which were observed by chemical ionization experiments, were structurally characterized by collisionally activated dissociation spectrometry, and their unimolecular decomposition processes were probed by mass-analyzed ion kinetic energy spectrometry. The results of these experiments are discussed in terms of the potential energy profile obtained by investigating the potential energy surfaces of singlet and triplet $(NF_2CO)^+$, as well as the hyperline corresponding to their intersection. Our findings provide probably the first detailed description of the mechanism of a formally simple F^+ transfer reaction. They also have mechanistic implications for related oxidative fluorination reactions in solution, which have been extensively investigated in the last thirty years.

Keywords: ab initio caculations · fluorine · gas-phase chemistry · ion–molecule reactions · mass spectrometry

Introduction

The formal transfer of F^+ between elementary neutral species N_1 and N_2 is a prototype reaction of general interest. Such processes involving monoatomic and simple polyatomic neutral species in solution have been extensively investigated in the last thirty years[1–8] and are already classic examples of the preparation and structural characterization of main group compounds. These studies have also stimulated considerable interest in the fundamental aspects of reactions (1), and this has resulted in detailed theoretical knowledge of the thermochemistry of the simplest F^+ transfer reactions.[1] Their detailed mechanisms are much less well understood. Gas-phase reactions involving monoatomic and diatomic neutral species[9, 10] may serve as simple models for studying these aspects. Following our recent observation of the gas-phase reaction of Equation (2),[9] we report here an experimental

$$N_1F^+ + N_2 \rightarrow N_2F^+ + N_1 \tag{1}$$

$$^1NF_2^+ + CO \rightarrow {}^1FCO^+ + {}^3NF \tag{2}$$

and theoretical study on its detailed mechanistic aspects. Our results contribute to general discussions of F^+ transfer in solution and to the study of spin-forbidden processes in the gas phase. These reactions are currently of considerable experimental[11] and theoretical[12] interest.

Results

The F^+ transfer reaction: thermochemical considerations: As part of our continuing interest in the gas-phase ion chemistry of NF_2^+,[13] we recently observed[9] a formal F^+ transfer reaction [Eq. (2)] by using Fourier transform ion cyclotron resonance (FT-ICR) spectrometry.[14] The NF_2^+ ions were prepared in the external source of the instrument by electron impact ionization of NF_3,[15] transferred into the resonance cell, isolated, thermalized by unreactive collisions with pulsed-in argon, and allowed to react with CO. The only ionic product observed was FCO^+, which was unambiguously identified by exact mass measurements, and the efficiency of the reaction was 0.02 from the ratio of the experimental rate constant and the collision rate constant, estimated as 7.67×10^{-10} cm^3 molecule^{-1} s^{-1} from average dipole orientation theo-

---

[*] Prof. F. Grandinetti
Dipartimento di Scienze Ambientali
Università della Tuscia
Via S. C. De Lellis, I-01100, Viterbo (Italy)
Fax: (+39) 761-357179
E-mail: fgrandi@unitus.it

Dr. M. Aschi[+]
Centro Studio C.N.R. per il Calcolo Intensivo in Scienze Molecolari
c/o Dipartimento di Chimica, Università di Perugia
Via Elce di Sotto, 8 Perugia (Italy)

Dr. V. Vinciguerra
Dipartimento di Agrobiologia ed Agrochimica
Università della Tuscia, Via S.C. De Lellis
I-01100, Viterbo (Italy)

[+] Permanent address: Dipartimento di Scienze Ambientali
Università della Tuscia
Via S.C. De Lellis, I-01100, Viterbo (Italy)

0947-6539/98/0411-2366 $ 17.50+.50/0

Table 1. Zero-point energies (ZPEs) and G2 and G2MS total energies [au] of NF_2^+, $F(CO)^+$, NF, and CO.

Species	ZPE(G2)	G2 (0 K)	G2 (298.15 K)	ZPE (G2MS)	G2MS (0 K)	G2MS (298.15 K)
NF_2^+ ($^1A_1$)	0.00886	– 253.58779	– 253.58484	0.00751	– 253.57260	– 253.56963
NF_2^+ ($^3B_1$)	0.00766	– 253.50053	– 253.49746			
FCO^+ ($^1\Sigma^+$)	0.01224	– 212.52311	– 212.52038	0.01105	– 212.51251	– 212.50976
FCO^+ ($^3A'$)	0.00782	– 212.33768	– 212.33460			
FOC^+ ($^1A'$)	0.00726	– 212.28540	– 212.28203			
FOC^+ ($^3A''$)	0.00602	– 212.29354	– 212.28922			
NF ($^3\Sigma^-$)	0.00300	– 154.27202	– 154.26964	0.00271	– 154.25726	– 154.25488
NF ($^1\Delta$)	0.00307	– 154.21066	– 154.20828	0.00280	– 154.20295	– 154.20058
CO ($^1\Sigma^+$)	0.00556	– 113.17750	– 113.17514	0.00503	– 113.17196	– 113.16960

ry.[16] Here we present more detailed considerations of the thermochemistry of reaction (2) and the electronic states of the involved ions and neutral species. They are based on experimental thermochemical data[17] and on calculations with the Gaussian-2 (G2) theory[18] and its modified version (G2MS)[19] (Table 1).

The NF_2^+ ions that underwent reaction (2) under FT-ICR conditions were preliminarily thermalized by unreactive collisions with argon, and their intensity was found to decrease exponentially over the entire time interval. This suggested[9] the exclusive formation of NF_2^+ ions in their electronic ground state, that is, $^1A_1$.[20] Additional thermochemical considerations confirm this conclusion. In particular, consistent with previous experimental[21] and theoretical[20b] estimates, our G2 energy difference between the $^1A_1$ state of NF_2^+ and its lowest energy excited state $^3B_1$ is about 2.4 eV. Taking the recombination energy of NF_2^+ in its ground state as approximately equal to the ionization potential (IP) of NF_2 (11.63 eV), electronically excited NF_2^+ ions should have a recombination energy of at least about 14.0 eV. Therefore, they should undergo appreciable near-resonant or exothermic electron capture from simple molecules such as CO (IP = 14.0 eV), N_2O (IP = 12.9 eV), and H_2O (IP = 12.6 eV). Such reactions were not observed in our previous experiments on the reactivity of thermalized NF_2^+ with such nucleophiles.[9, 13e, c] However, we observed highly efficient electron transfer on reacting thermalized NF_2^+ with HN_3 (IP = 10.72 eV)[13g] and H_2NCN (IP ≈ 10.4 eV).[13f]

Abstract in Italian: *Il presente lavoro riporta i risultati di uno studio dettagliato, effettuato mediante spettrometria di massa e calcoli teorici di tipo DFT ed ab initio, del meccanismo della reazione di formale trasferimento di* F^+ *da parte dello ione* $^1NF_2^+$ *alla molecola di CO con formazione dello ione* $^1F\text{-}CO^+$ *e del radicale* ^3NF*. In questo processo spin-proibito sono coinvolti quali intermedi gli ioni* $(NF_2CO)^+$*. Essi sono stati osservati mediante esperimenti di ionizzazione chimica e caratterizzati nella loro struttura e nei loro processi di decomposizione unimolecolare mediante spettrometria CAD e MIKE. I risultati di questi esperimenti sono stati discussi in termini del profilo di energia potenziale relativo agli ioni* $(NF_2CO)^+$*, studiato sia nelle regioni adiabatiche del singoletto e del tripletto che nella regione corrispondente alla intersezione di queste due superfici. I risultati di questo studio hanno consentito quella che costituisce probabilmente la prima descrizione dettagliata del meccanismo di una reazione di formale trasferimento di* F^+*. Inoltre, essi forniscono lo spunto per alcune considerazioni di carattere generale riguardanti i processi di fluorurazione ossidativa che avvengono in soluzione e che sono stati approfonditamente studiati nel corso degli ultimi trenta anni.*

The electronic state and the connectivity of the products of reaction (2) can be safely assigned as $^1FCO^+$ and ^3NF. According to Table 1, the formation of any other pair of products, including $^1FCO^+$ and ^1NF, in the reaction between $^1NF_2^+$ and CO would be significantly endothermic and should not be observed to any appreciable extent under the conditions of the FT-ICR experiments. Assuming a target accuracy of the G2 calculations of about 2.5 kcal mol^{-1}[18] at 298.15 K the formation of $^1FCO^+$ and ^3NF from reaction (2) is predicted to be exothermic by 18.9 ± 2.5 kcal mol^{-1}. This is consistent with the experimental value of 15.0 ± 3.0 kcal mol^{-1} obtained by using the enthalpy of formation of FCO^+, which was recently determined as 178.1 ± 2.3 kcal mol^{-1} by photoionization mass spectrometry.[22] We reevaluated this enthalpy change by the G2MS procedure, which is significantly less elaborate than G2 but in principle of comparable accuracy.[19] The value of 16.0 ± 2.5 kcal mol^{-1} obtained from Table 1 provides support for the application of G2MS in the investigation of the $(NF_2CO)^+$ ions that are conceivably involved in reaction (2). Finally, we note that the G2 energy gap of 38.5 kcal mol^{-1} between the $^3\Sigma^-$ ground state and the $^1\Delta$ excited state of NF[23] is slightly larger than a previous estimate of 31.4 kcal mol^{-1}, which was based on large-scale MRD-CI ab initio calculations.[24] In addition, at the G2 level of theory, the singlet FCO^+ isomer is more stable than the triplet by more than 116 kcal mol^{-1}, but the triplet FOC^+ isomer is more stable than the singlet by 4.5 kcal mol^{-1}.

The $(NF_2CO)^+$ adducts: experimental observation and structural characterization: The $(NF_2CO)^+$ intermediates conceivably involved in reaction (2) but not observed in the low-pressure domain of the FT-ICR experiments ($p \approx 10^{-7}$ mbar) were instead detected by ionization of NF_3/CO mixtures introduced into the higher pressure domain of chemical ionization (CI) sources ($p \approx 10^{-2}$ mbar) of the VG-TS 250 and the ZAB-2F[25] spectrometers. In addition, the intensity of these ions in the CI source of the ZAB-2F instrument was high enough to allow their structural characterization by collisionally activated dissociation (CAD)[26] and mass-analyzed ion kinetic energy (MIKE)[27] spectrometry.

The results of the MIKE experiments were particularly informative. The MIKE spectrum of the $(NF_2CO)^+$ ions consisted exclusively of FCO^+ ($m/z = 47$), which corresponds to the loss of neutral NF. This provides unambiguous evidence for the intermediacy of $(NF_2CO)^+$ in reaction (2). Even more interesting was the shape of the MIKE peak (Figure 1). Although the MIKE spectrum was recorded at the relatively low resolution of about 5000, due to the low intensity of the metastable transition, the composite shape of the peak can be clearly seen. It consists of a narrow central component and a large, probably flat-topped component with a kinetic energy release (KER) of 272 meV at the half-height of the peak ($E_{t½}$). Relatively large KERs and non-Gaussian peak shapes generally indicate unimolecular decompositions with high reverse activation energies and are typical of fragmentation processes that require prior rearrangement of the decomposing ions. In contrast, processes such as direct bond cleavage (continuously endothermic) have little or no reverse activation energy and usually give rise to small KERs and narrow Gaussian-type peaks.[27, 28]

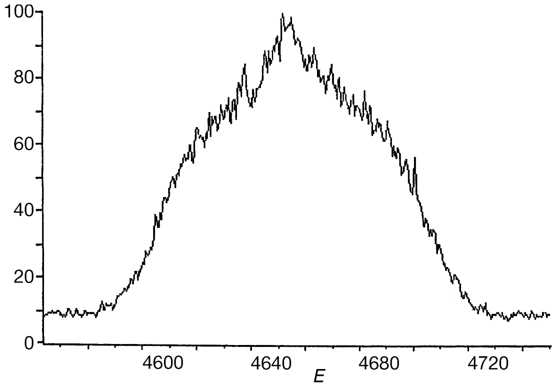

Figure 1. MIKE peak of the decomposition reaction $(NF_2CO)^+ \rightarrow FCO^+ + NF$. E = energy.

The CAD spectrum of the $(NF_2CO)^+$ ions (Table 2) confirms their elemental composition. In addition, the intense peak for the NF_2^+ fragment at $m/z = 52$ is of particular interest since it is structurally diagnostic of an ionic population of connectivity $NF_2^+-(CO)$. However, the observed fragmentation pattern is not inconsistent with alternative structures. In particular, keeping in mind the results of our theoretical calculations (vide infra), we draw attention to the possible formation of $FCO^+-(NF)$ isomers.

Table 2. CAD spectroscopic data of the $(NF_2CO)^+$ ions.

m/z	Fragment	Relative intensity
61	$FNCO^+$	6.1
52	NF_2^+	100
47	FCO^+	25.1
45	FCN^+	0.9
42	NCO^+	3.0
33	NF^+	16.6
31	CF^+	2.2
28	CO^+	10.3
14	N^+	1.1
12	C^+	1.0

Theoretical investigation of the NF_2^+-(CO) and FCO^+-(NF) isomers: structure, stability, and interconversion: We performed DFT and ab initio calculations to investigate the structure, stability, and interconversion of the $NF_2^+-(CO)$ and $FCO^+-(NF)$ intermediates conceivably involved in the spin-forbidden reaction (2). First we searched for the $NF_2^+-(CO)$ and $FCO^+-(NF)$ energy minima on the singlet and triplet B3LYP/6-31G(d) potential enrgy surfaces (PESs). We found the four isomers **1S**–**4S** on the singlet PES, and the three isomers **1T**–**3T** on the triplet PES. The structures of these ions are shown in Figure 2, and their geometric data are listed in Table 3. The relevant data for the evaluation of their G2MS total energies are collected in Table 4.

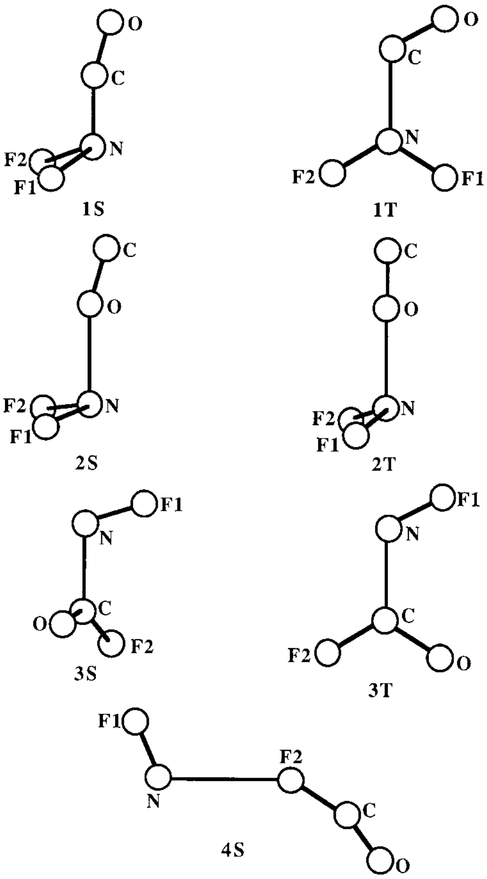

Figure 2. B3LYP/6-31G(d) connectivities of **1S**–**4S** and **1T**–**3T**.

The isomers **1S** and **2S** must be viewed as the C- and O-bonded complexes of $^1NF_2^+$ with CO. The calculated distances between the two moieties of 1.352 Å in **1S** and 2.326 Å in **2S** are significantly different and suggest an appreciable difference in the stability of these two isomers with respect to separation into $^1NF_2^+$ and CO. Consistently, at the G2MS level of theory and 298.15 K with the total entropies derived from the B3LYP/6-31G(d) frequencies and moments of inertia, the formation of **1S** from $^1NF_2^+$ and CO is exothermic by $26.1 \pm 2.5\,kcal\,mol^{-1}$ and exoergic by $15.9 \pm 2.5\,kcal\,mol^{-1}$.[29] In contrast, the formation of **2S** is exothermic by $5.5 \pm 2.5\,kcal\,mol^{-1}$ but endoergic by $2.7 \pm 2.5\,kcal\,mol^{-1}$. This finding is of considerable importance for the discussion of the detailed mechanism of reaction (2). We can assume that at 298.15 K the association of thermalized $^1NF_2^+$ with CO, which conceivably occurs in the first elementary step, leads to almost

Table 3. B3LYP/6-31G(d) optimized parameters of **1S**–**4S** and **1T**–**3T** (for atom numbering scheme, see Figure 2).

Species	Bond length [Å]		Bond angle [°]		Dihedral angle [°][a]	
1S (C_s)	C–N	1.352	N-C-O	164.4	F1-N-C-O	118.1
	C–O	1.130	C-N-F1	111.5		
	N–F1	1.351				
2S (C_s)	N–O	2.326	N-O-C	170.1	F1-N-O-C	125.7
	C–O	1.148	O-N-F1	99.4		
	N–F1	1.274				
3S (C_1)	C–N	1.437	C-N-F1	109.0	O-C-N-F1	98.7
	C–O	1.205	N-C-O	94.4	F2-N-C-F1	– 83.0
	N–F1	1.295	N-C-F2	129.7		
	C–F2	1.258				
4S (C_1)	N–F1	1.279	F1-N-F2	112.2	F1-N-F2-C	178.9
	N–F2	2.593	N-F2-C	142.4	N-F2-C-O	– 0.3
	C–F2	1.236	F2-C-O	163.5		
	C–O	1.134				
1T (C_s)	C–N	1.932	N-C-O	132.5		
	C–O	1.129	C-N-F1	127.0		
	N–F1	1.308	C-N-F2	120.0		
	N–F2	1.301				
2T (C_s)	N–O	2.491	N-O-C	179.9	F1-N-O-C	123.1
	C–O	1.140	O-N-F1	123.1		
	N–F1	1.307				
3T (C_s)	C–N	1.627	C-N-F1	118.1		
	C–O	1.168	N-C-O	116.3		
	N–F1	1.268	N-C-F2	104.9		
	C–F2	1.262				

[a] Negative values indicate anticlockwise rotations.

exclusive formation of the intermediate **1S**. We note that the preferred coordination of the Lewis acid $^{1}\mathrm{NF}_2^+$ to the C atom of CO is in line with the results of recent studies on the relative stability of the isomeric ions arising from the coordination of CO with a number of isolated cations.[30]

Changing the multiplicity from singlet to triplet strongly affects the structure and stability of the NF_2^+–(CO) ions. The isomers **1T** and **2T** are complexes between $^{3}\mathrm{NF}_2^+$ and CO with long distances between the two moieties. They are of comparable stability and less stable than **1S** by 47.4 and 44.7 kcal mol^{-1}, respectively. Both **3S** and **4S** must be regarded as complexes between $^{1}\mathrm{FCO}^+$ and $^{1}\mathrm{NF}$. However, they differ significantly in structure and stability. Isomer **3S** is more stable than **1S** by 2.2 kcal mol^{-1} and it is the global minimum on the singlet PES. It is also the most stable of the various investigated singlet and triplet isomers. Consistent with its relatively short C–N distance (1.437 Å), the G2MS enthalpy change for its formation from separate $^{1}\mathrm{FCO}^+$ and $^{1}\mathrm{NF}$ is 46.4 ± 2.5 kcal mol^{-1} at 298.15 K (Tables 1 and 4). Isomer **4S** is a high-energy minimum, 47.5 kcal mol^{-1} less stable than **1S**. Isomer **3T** is the global minimum on the triplet PES, but it is less stable than **3S** by 6.6 kcal mol^{-1}. In spite of their similar connectivities, **3S** and **3T** significantly differ in their detailed structure. In particular, isomer **3T** is fully planar, and its C–N distance of 1.627 Å is significantly longer than that of **3S**. Finally, we have not found any energy minimum of connectivity similar to **4S** on the triplet PES.[31]

Reaction (2) conceivably commences by addition of $^{1}\mathrm{NF}_2^+$ to CO with formation of the isomer **1S** on the singlet PES, and the eventually observed products $^{1}\mathrm{F\text{-}CO}^+$ and $^{3}\mathrm{NF}$ conceivably arise from the dissociation of **3T** on the triplet PES. Therefore, a proper discussion of the mechanism of the overall reaction (2) requires detailed knowledge of all the conceivable reaction paths that connect **1S** and **3T**. These spin-forbidden processes could occur directly or involve the intermediacy of one or more of the various isomers on the singlet and triplet PESs. However, general considerations suggest that only **3S** can play an active role in the mechanism of reaction (2). In fact, according to the double-well potential model of ion–molecule reactions,[32] the observation of the overall reaction (2) for thermalized $^{1}\mathrm{NF}_2^+$ ions at a rate measurable under FT-ICR conditions indicates that the free energies of the structures which interconnect the isomers conceivably involved in its various elementary steps are not appreciably higher than the ($^{1}\mathrm{NF}_2^+ + \mathrm{CO}$) entrance channel. The isomers **4S**, **1T**, and **2T** are significantly less stable than this limit (Table 4), and the structures which lead to their formation from the more stable isomers must be at least equal in energy. Therefore, we can rule out their intermediacy in reaction (2) and focus exclusively on the formation of **3S.**

Whereas locating the transition state (TS) which connects **1S** and **3S** on the singlet PES is in principle relatively straightforward, finding the structures that connect species such as **1S** and **3T** or **3S** and **3T**, which lie on PESs of different electron multiplicity, is more challenging. According to a nonrelativistic approach in the Born–Oppenheimer approximation, these spin-forbidden interconnections can be described as transitions from two energy minima that lie on two different noninteracting PESs. These nonadiabatic processes can occur only in the vicinity of the crossing hyperline, that is, the zone of intersection of the two noninteracting surfaces, where they are induced mainly by spin–orbit coupling (SOC) between the two PESs.[12a] By oversimplified analogy with the transition state theory of unimolecular reactions on a single

Table 4. Absolute energies and corrections [au] for the evaluation of the G2MS total energies of **1S**–**4S** and **1T**–**3T**, NF_2^+, and CO fragments. The relative enthalpies at 298.15 K ΔH values are given in kcal mol^{-1}.

Species	B3LYP/6-31G(d)	CCSD(T)/6-31G(d)	Δ(MP2)	HLC	ZPE	G2MS (0 K)	G2MS (298.15 K)	ΔH
1S ($^{1}A'$)	– 367.19897	– 366.33433	– 0.38211	– 0.08358	0.01689	– 366.78313	– 366.77847	0.0
2S ($^{1}A'$)	– 367.16624	– 366.30973	– 0.37239	– 0.08358	0.01386	– 366.75184	– 366.74570	20.6
3S	– 367.20531	– 366.34066	– 0.37937	– 0.08358	0.01713	– 366.78648	– 366.78190	– 2.2
4S	– 367.12505	– 366.25780	– 0.38136	– 0.08358	0.01335	– 366.70939	– 366.70280	47.5
1T ($^{3}A''$)	– 367.13718	– 366.26869	– 0.37648	– 0.07799	0.01429	– 366.70887	– 366.70299	47.4
2T ($^{3}A''$)	– 367.11201	– 366.22877	– 0.41964	– 0.07799	0.01247	– 366.71393	– 366.70726	44.7
3T ($^{3}A''$)	– 367.20853	– 366.33599	– 0.37829	– 0.07799	0.01585	– 366.77642	– 366.77142	4.4
NF_2^+ ($^{1}A_1$)	– 253.83704	– 253.25966	– 0.26671	– 0.05373	0.00751	– 253.57259	– 253.56963	+ 26.1
CO ($^{1}\Sigma^+$)	– 113.30945	– 113.03796	– 0.10918	– 0.02985	0.00503	– 113.17196	– 113.16960	
FCO ($^{1}\Sigma^+$)	– 212.75039	– 212.25639	– 0.21941	– 0.04776	0.01105	– 212.51251	– 212.50976	+ 10.2
NF ($^{3}\Sigma^-$)	– 154.43592	– 154.07744	– 0.15827	– 0.02426	0.00271	– 154.25726	– 154.25488	

0947-6539/98/0411-2369 $ 17.50+.25/0

Table 5. B3LYP/6-31G(d) optimized geometries, zero-point energies (ZPEs), and total energies [au] of the **TSS**, **MECP1**, **MECP2**, and **MECP3** structures (for atom numbering scheme, see Figure 3).

Species	Bond length [Å]		Bond angle [°]		Dihedral angle [°][a]		ZPE	B3LYP/6-31G(d)
TSS (C_1)	C–N	1.416	C-N-F2	62.2	F1-N-C-O	93.6	0.01561	– 367.17082
	C–F2	1.605	F1-N-C	109.7	F2-N-C-O	– 167.5		
	N–F1	1.305	N-C-O	160.4				
	N–F2	1.665						
	C–O	1.137						
MECP1 (C_1)	C–N	1.342	C-N-F2	91.3	F1-N-C-O	137.0		– 367.11600
	C–F2	2.469	F1-N-C	111.8	F2-N-C-O	– 106.5		
	N–F1	1.326	N-C-O	168.3				
	N–F2	2.042						
	C–O	1.136						
MECP2 (C_1)	N–F1	1.276	F1-N-F2	107.8	F1-N-F2-C	89.7		– 367.11750
	N–F2	1.491	N-F2-C	175.1	N-F2-C-O	0.0		
	C–F2	1.996	F2-C-O	178.7				
	C–O	1.126						
MECP3 (C_1)[b]	C–N	1.514 (1.529)	C-N-F1	111.6 (112.3)	O-C-N-F1	63.1 (63.0)	0.01490	– 367.19600 (– 366.32500)
	N–F1	1.273 (1.273)	N-C-O	112.8 (113.7)	F2-C-N-F1	– 124.8 (– 124.0)		
	C–F2	1.270 (1.270)	N-C-F2	112.1 (111.0)				
	C–O	1.182 (1.179)						

[a] Negative values indicate anticlockwise rotations. [b] CCSD(T)/6-31G(d)//B3LYP/6–31G(d) data in parentheses.

PES, the system must overcome the minimum of the above hyperline (defined as the minimum energy crossing point, MECP), which can be regarded as a sort of transition state.[12c] However, the reaction will effectively take place at the MECP only if the SOC term, which plays the same role as the transmission coefficient,[33] is nonzero and allows switching from the reactant PES to the product PES. Therefore, according to this approximate approach, the rate of a nonadiabatic process can be estimated by determining the position of the MECP and the corresponding spin–orbit coupling matrix element. Several methods are available for locating the MECP.[34] We employed a hybrid approach that was recently used to investigate the nonadiabatic chemistry of the phenyl cation.[35] The detailed theoretical and computational aspects are given in ref. [35] and are summarized in this paper (see Experimental Section and Methods of Calculation). Here we simply report the results of its application to the present system.

The connectivities of the located TSs and MECPs are shown in Figure 3, and their detailed geometries and energies are reported in Table 5. On the singlet PES, the interconversion of the isomers **1S** and **3S** passes through the transition state structure **TSS**. At the B3LYP/6-31G(d) level, this species has a single imaginary frequency of 386.4 i cm^{-1}, which formally refers to the migration of the fluorine atom from nitrogen to carbon. The N–F2 and C–F2 bond lengths of this bridged fluoronium ion of 1.665 and 1.605 Å, respectively, are appreciably longer than the corresponding bond lengths of **1S** and **3S** (1.259 and 1.210 Å, respectively), and significant structural rearrangement is required to overcome the activation barrier. Consistently, at the G2MS level of theory,[36] the activation barrier is as high as 19.1 kcal mol^{-1} with respect to **1S**. By moving along the reaction path formally visualized as a 1,2-fluorine migration from the nitrogen to the carbon atoms of isomer **1S**, we also located the minimum energy crossing point **MECP1**. In addition, we found the crossing point **MECP2** by following the reaction path which can be formally visualized as a colinear transfer of F$^+$ from $^1NF_2^+$ to CO. Both **MECP1** and **MECP2** allow, in principle, the direct interconnection of **1S** and **3T**. Although their connectivities and detailed geometries are quite different, their B3LYP/6-31G(d) total energies differ by only 1 kcal mol^{-1}. Most importantly, at the same computational level they are less stable than **TSS** by more than 33 kcal mol^{-1}. Therefore (vide infra), they should not play any active role in the mechanism of reaction (2) and we refrained from calculating the corresponding zero-point energies and SOC.

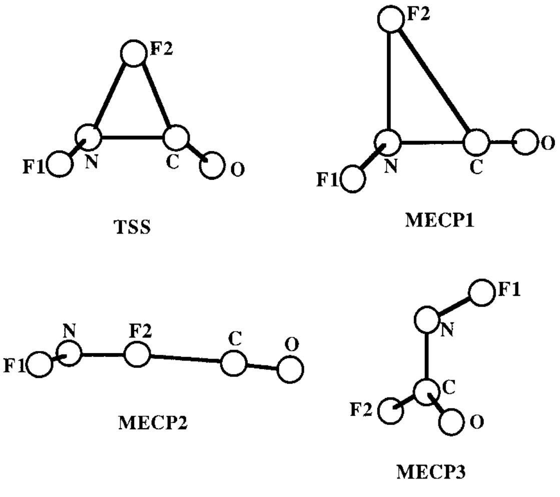

Figure 3. B3LYP/6-31G(d) connectivities of **TSS**, **MECP1**, **MECP2**, and **MECP3**.

The minimum energy crossing point **MECP3** connects **3S** and **3T**. From Tables 3 and 5, this process formally occurs by rotation of the FCO group around the C–N bond and bending of the N-C-O angle. At the B3LYP/6-31G(d) level and 0 K, **MECP3** is less stable than **1S** by only 0.6 kcal mol^{-1}. Since this structure plays a crucial role in the mechanism of reaction (2), we refined its geometry and total energy at the CCSD(T)/6-31G(d)//B3LYP/6-31G(d) level. The geometrical parameters do not change appreciably (Table 5), and the energy difference with **1S** is 4.6 kcal mol^{-1}. The absolute value of the SOC at **MECP3** is 59 cm^{-1}. The CCSD(T)/6-31G(d)//B3LYP/6-31G(d) relative energies of **1S**, **3S**, **3T**, and their interconnecting structures at 0 K are shown schematically in Figure 4.

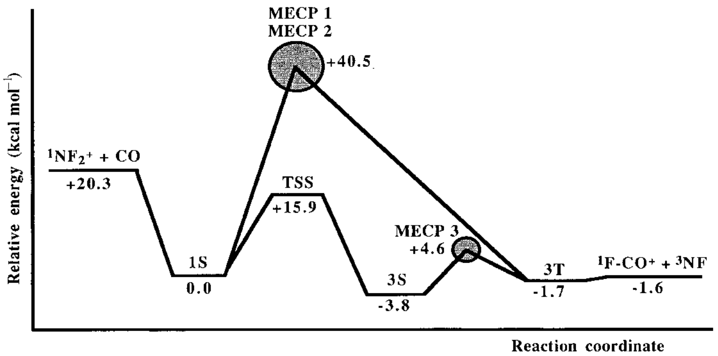

Figure 4. CCSD(T)/6-31G(d)//B3LYP/6-31G(d) relative energy at 0 K of the $(NF_2CO)^+$ isomers and their dissociation products. The values for **MECP1** and **MECP2** are the B3LYP/6-31G(d) relative energies without ZPE.

Discussion

Mechanistic aspects of the F^+ transfer reaction: The theoretical and mass spectrometric results both provide evidence for the reaction sequence of Equations (2a)–(2d) as the detailed mechanism of the gas-phase F^+ transfer reaction (2). The

$$^1NF_2^+ + CO \rightarrow \mathbf{1S} \qquad (2a)$$

$$\mathbf{1S} \rightarrow [\mathbf{TSS}] \rightarrow \mathbf{3S} \qquad (2b)$$

$$\mathbf{3S} \rightarrow [\mathbf{MECP3}] \rightarrow \mathbf{3T} \qquad (2c)$$

$$\mathbf{3T} \rightarrow {}^1F\text{-}CO^+ + {}^3NF \qquad (2d)$$

process commences with the exothermic and exoergic addition of $^1NF_2^+$ to CO with formation of the C-bonded isomer **1S**. In the low-pressure domain of the FT-ICR experiments, this intermediate from reaction (2a), which is excited by the exothermicity of its formation process and is not stabilized by unreactive collisions with surrounding molecules, can dissociate back into the reactants or, at least in principle, overcome the barriers corresponding to **TSS**, **MECP1**, or **MECP2**. However, the energies of the two singlet-to-triplet crossing points are significantly higher than the energy of the separate reactants $^1NF_2^+$ and CO (Figure 4). Therefore, according to the double-well potential model,[32] the only energy barrier which can allow the consumption of $^1NF_2^+$ ions at a rate measurable under FT-ICR conditions is the adiabatic barrier corresponding to **TSS**. According to Figure 4, the $^1F\text{-}CO^+\text{-}(^1NF)$ intermediate **3S** is formed in reaction (2b) with sufficient energy to overcome the crossing point **MECP3** and transform into **3T** [Eq. (2c)], which in turn can undergo barrier-free dissociation [Eq. (2d)] to give the observed products $^1FCO^+$ and ^3NF. According to the sequence 2a–d and Figure 4, the efficiency of the overall process [Eq. (2)] depends on the kinetic competition between the entropically favored back dissociation of **1S** into $^1NF_2^+$ and CO and its enthalpically favored isomerization into **3S**, as well as on the probability that **3S** can overcome the singlet-to-triplet crossing point **MECP3**. Our theoretical findings suggest that the low experimental value of 0.02 arises essentially from the former of these two factors. In fact, at the G2MS level of theory and 298.15 K the free energy change of 15.9 ± 2.5 kcal mol^{-1} for the dissociation of **1S** into $^1NF_2^+$ and CO is practically identical, within the combined uncertainties of the G2MS calculations, with the free energy difference of 19.5 ± 2.5 kcal mol^{-1} between **TSS** and **1S** (the entropy of **TSS** was estimated from the corresponding B3LYP/6-31G(d) frequencies and moments of inertia). This is expected to result[32] in a rather slow reaction (2b). In contrast, the value of the SOC calculated for **MECP3** is small, as expected for species containing only light atoms,[12a] but large enough to ensure a fast transition from the singlet to the triplet surface in elementary step (2c).

The results of the CI, CAD, and MIKE experiments are consistent with the reaction sequence 2a–d and provide additional evidence for the potential energy profile depicted in Figure 4. In the relatively high pressure domain of CI sources, the intermediate **1S** from (2a) can be partially stabilized by unreactive collisions with the bath gases and observed to an appreciable extent. The observation of an intense peak for the NF_2^+ fragment in the CAD spectrum of the $(NF_2CO)^+$ ions is fully consistent with the formation, not necessarily exclusive, of an adduct between NF_2^+ and CO. Most significantly, Figure 4 provides a satisfactory explanation for the details of the MIKE peak shown in Figure 1. In particular, the flat-topped component can be assigned to ions **1S** that overcome the isomerization barrier corresponding to the transition structure **TSS** and eventually dissociate into $^1FCO^+$ and ^3NF. The energy difference (G2MS, 298.15 K) of 10.4 kcal mol^{-1} (0.451 eV) between **TSS** and the dissociation products is partially released as kinetic energy of the fragments, and the remainder is partitioned between their rotational and/or internal degrees of freedom. This is consistent with the experimentally observed $E_{t1/2}$ of 272 meV. In addition, taking into account the evidence from the study of a large number of simple ions,[37] this value should exceed the mean kinetic energy release by about 15–20 %. Therefore, we estimate that the mean kinetic energy of the $^1FCO^+$ and ^3NF fragments of about 220 meV amounts to about 49 % of the energy difference between **TSS** and $(^1FCO^+ + {}^3NF)$ at the G2MS level. This finding is in line with our previous results for the unimolecular decomposition of related cations. For example, the mean kinetic energies of the fragments arising from the unimolecular reactions of Equations (3)–(5) accounted for about 56,[13b] 62,[13c] and 46 %,[13g] respectively, of

$$FN\text{-}OH^+ \rightarrow NO^+ + HF \qquad (3)$$

$$NF_2\text{-}OH_2^+ \rightarrow FN\text{-}OH^+ + HF \qquad (4)$$

$$NF_2\text{-}NH^+ \rightarrow FN_2^+ + HF \qquad (5)$$

the calculated energy differences between the transition states and the dissociation products. The narrow component of the MIKE peak in Figure 1 indicates a dissociation process with a negligible release of kinetic energy. This likely reflects the structurally inhomogeneous character of the $(NF_2CO)^+$ ionic population generated in the CI source by ionization of NF_3/CO mixtures. As a simple explanation, we assign this component to ions of connectivity **3S** and/or **3T.** According to Figure 4, the dissociation of both of these species is expected to occur with negligible KER. The mixed character of the $(NF_2CO)^+$ ionic population that is clearly indicated by the results of the MIKE experiments is not inconsistent with the fragmentation pattern in their CAD spectrum. For example, it is of interest to note the relatively intense peak for the NF^+ fragment at $m/z = 33$.

The transition structure **TSS** involved in elementary step (2b) plays a crucial role in the formal F^+ transfer reaction (2). It is a bridged fluoronium ion whose imaginary frequency refers to a 1,2-fluorine migration. Therefore, we can regard reaction (2) as one of the few gas-phase ion–molecule reactions which involve a 1,2-fluorine shift as a key elementary step. The possible occurrence of this process in the gas phase has often been suggested,[38] but it has been documented only in a few cases.[39]

Implications for the mechanism of oxidative fluorination in solution: The processes which are more strictly related to our gas-phase reaction [Eq. (2)] are undoubtedly the oxidative fluorinations in solution that involve monoatomic and simple polyatomic neutral species. Most of these F^+ transfer reactions, intensively investigated in the last three decades,[2–8] have been recently put in the perspective by the theoretical development of the first quantitative scale for the oxidizing strength of oxidative fluorinating agents NF^+.[1] The thermochemistry of the reactions was invariably consistent with the rankings on the scale, and the position of each oxidizing agent was related to its geometry and to the oxidation state, the electronegativity, and the electron lone pairs of the central atom. However, the detailed mechanisms of even the simplest oxidative fluorination reactions in solution are much less well understood and are complicated by the effects of the solvent, the counterions, and catalysts, etc. As a further example of the ability of gas-phase ion chemistry to provide a means for investigating aspects which may be difficult to study in solution, our results indicate that gas-phase studies can in principle provide detailed information on the reaction path in a formally simple F^+ transfer reaction. In addition, certain processes which occur in solution are analogous to reaction (2). For example, we note the formal analogy with the exothermic F^+ transfer reaction of Equation (6), which is an

$$FN_2^+AsF_6^- + ClF \rightarrow ClF_2^+AsF_6^- + N_2 \qquad (6)$$

exemplary case of oxidative fluorination.[4d] The fluorodiazonium ion FN_2^+ is an electron-deficient species like $^1NF_2^+$, and ClF is a simple diatomic molecule like CO. Based on our findings on the mechanistic details of reaction (2), we perceive the formal F^+ transfer from N_2 to ClF as involving the initial formation of an intermediate FN_2ClF^+ complex, which subsequently undergoes a 1,2-fluorine shift and forms N_2 and ClF_2^+ as the eventual reaction products. On the other hand, the formal F^+ transfer from a saturated oxidizing agent such as NF_4^+ to a Lewis base B should probably involve an intermediate or a transition state with a colinear arrangement of the fluorine atom between the nitrogen atom of NF_4^+ and the base B.

Conclusions

The detailed investigation of the gas-phase reaction (2) convincingly supports the conclusion that even the formally simplest F^+ transfer reactions conceivably involve complex reaction paths in which several distinct intermediates and interconnecting structures participate. It would be therefore of considerable interest to investigate the actual existence of these species and to elucidate their detailed mechanistic role. In addition, our findings suggest that the simplest spin-forbidden F^+ transfer reactions may serve as useful models to investigate the general aspects of spin-forbidden ion–molecule reactions in the gas phase. In this respect, the recent experimental and theoretical investigation of spin-forbidden proton transfers[11b, c] and of simple organometallic reactions which conceivably occur by two-state reactivity[11a, 12e] have already proved to be of general interest.

Experimental Section and Methods of Calculation

The $(NF_2CO)^+$ ions were prepared by introducing a NF_3/CO mixture (typical ratio ca. 2/1) into the CI source of a VG-TS 250 spectrometer in the electrostatic/magnetic (E/B) configuration. Typical operating conditions of the source were as follows: bulk-gas pressure about 10^{-2} mbar, source temperature 160 °C, emission current 300 mA, trap current 35 μA, electron energy 35 eV, repeller voltage 11 V, accelerating voltage 4 kV.

The MIKE and CAD spectra of the $(NF_2CO)^+$ ions were recorded in a VG Micromass ZAB-2F instrument in the magnetic/electrostatic (B/E) configuration.[25] Typical operating conditions of the CI source were as follows: bulk-gas pressure about 10^{-1} mbar, source temperature 150 °C, emission current 1 mA, electron energy 50 eV, repeller voltage about 0 V. The MIKE spectra were recorded with an accelerating voltage of 8 kV and an energy resolution ($E/\Delta E$) of $(3-5) \times 10^3$ and were averaged for at least 40 scans. The CAD spectra were recorded by admitting helium into the collision cell at a pressure that reduced the main beam intensity to about 70% of its initial value.

The G2 calculations[18] on NF_2^+, the $F(CO)^+$ isomers, NF, and CO were performed with the standard G2 routine implemented in the Gaussian 94 package of programs.[40] The geometries of **1S**–**4S**, **1T**–**3T**, and **TSS** were optimized at the DFT level of theory by using the B3LYP hybrid functional[41] in conjunction with the 6-31G(d) basis set.[42] The optimizations were initially performed without any symmetry constraint, and the unrestricted formalism was employed for the triplets. Critical points on the singlet and triplet PESs were unambigously characterized as minima or transition states by computing the corresponding analytical second derivatives matrix. The G2MS total energies of these species were computed according to the procedure described in ref. [19a]. Briefly, the B3LYP/6-31G(d) geometries are used in single-point calculations at the coupled-cluster[43] and Møller–Plesset[44] levels of theory to obtain the G2MS energy at 0 K according to Equation (7). The additive corrections were computed with the 6-311+G(2df, 2p) basis set[45] and are defined by Equation (8), where $HLC = -0.19n_\alpha - 5.78n_\beta$ (n_α and n_β are the number of α and β valence electrons ($n_\alpha \leq n_\beta$)) and ZPE is the B3LYP/6-31G(d) zero-point vibrational energy.

$$\text{G2MS (0 K)} = E[\text{CCSD(T)/6-31G(d)}] + \Delta(\text{MP2}) + \text{HLC} + \text{ZPE} \qquad (7)$$

$$\Delta(\text{MP2}) = E[\text{MP2/6-311+G(2df, 2p)}] - E[\text{MP2/6-31G(d)}] \qquad (8)$$

All single-point calculations included the valence electrons only (frozen-core approximation). The G2MS energy at 0 K was subsequently corrected at 298.15 K by adding the translational ($3RT/2$), rotational (RT or $3RT/2$ for linear and nonlinear species, respectively), and vibrational contributions at this temperature. The last term is calculated by standard statistical mechanics[46] formulas with the unscaled B3LYP frequencies. The calculated energy differences are converted to enthalpy differences by assuming ideal gas behavior and adding the appropiate ΔnRT contribution.

The minimum energy crossing points **MECP1**, **MECP2**, and **MECP3** between the isomers **1S**, **3S**, and **3T** on the B3LYP/6-31G(d) singlet and triplet PESs were located by a standard steepest descent approach[47] based on B3LYP/6-31G(d) electronic energies and analytical gradients. The location of **MECP3** was also refined at the CCSD(T)/6-31G(d)//B3LYP/6-

31G(d) level by using CCSD(T)/6-31G(d) energies and B3LYP/6-31G(d) gradients. The subsequent characterization of **MECP3** and the calculation of its frequencies was performed at the B3LYP/6-31G(d) level of theory by generating the corresponding effective Hessian matrix,[48] projecting the six rotations and translations as well as the direction perpendicular to the hyperline[49] and diagonalizing it to obtain the $3N-7$ nonzero positive force constants. The calculation of the off-diagonal SOC matrix elements between the singlet and all the substates of the triplet at **MECP3** was performed on the B3LYP/6-31G(d) geometry with CASSCF wavefunctions in conjunction with the TZV quality basis set (10s6p/5s3p).[50] The active space consisted of four electrons in four orbitals. The singlet wavefunction was fully optimized, and the triplet wavefunction was obtained by imposing the condition that its core orbitals be identical to those of the singlet.[35] An approximate one-electron operator[51] was used with an effective nuclear charge Z_{eff}[52] that was empirically adjusted to take into account the contribution of the missing two-electron term.

The CASSCF/SOC calculations as well as the projection of the effective Hessian matrix were performed using the Gamess program.[53] All other calculations were performed with Gaussian 94. We used the Linux versions of these packages installed on a Pentium PRO-S/200 machine and the parallel Unix version of Gaussian 94 installed on DEC AS4100 machines.

Acknowledgments: Financial support by the Italian Ministero dell' Università e della Ricerca Scientifica e Tecnologica (MURST) and the Consiglio Nazionale delle Ricerche (CNR) is gratefully acknowledged. We wish to thank Dr. F. Pepi (Università La Sapienza, Rome) for measuring the CAD and MIKE spectra and Dr. N. Sanna (CASPUR, Rome) for his skilful assistance in the installation of the program packages. M. A. wishes to thank CNR for a scholarship.

Received: April 22, 1998 [F 1113]

---

[1] K. O. Christe, D. A. Dixon, *J. Am. Chem. Soc.* **1992**, *114*, 2978.

[2] H. Meinert, U. Gross, *Z. Chem.* **1968**, *8*, 345.

[3] D. E. McKee, C. J. Adams, A. Zalkin, N. Bartlett, *J. Chem. Soc. Chem. Commun.* **1973**, 26.

[4] a) K. O. Christe, R. D. Wilson, *Inorg. Nucl. Chem. Lett.* **1973**, *9*, 845; b) K. O. Christe, W. W. Wilson, E. C. Curtis, *Inorg. Chem.* **1983**, *22*, 3056; c) K. O. Christe, W. W. Wilson, R. D. Wilson, *Inorg. Chem.* **1984**, *23*, 2058; d) K. O. Christe, R. D. Wilson, W. W. Wilson, R. Bau, S. Sukumar, D. A. Dixon, *J. Am. Chem. Soc.* **1991**, *113*, 3795.

[5] L. Stein, *Chemistry* **1974**, *47*, 15.

[6] a) R. J. Gillespie, G. J. Schrobilgen, *J. Chem. Soc.* **1974**, *13*, 1230; b) J. H. Holloway, G. J. Schrobilgen, *J. Chem. Soc. Chem. Commun.* **1975**, 623.

[7] a) V. B. Sokolov, Y. V. Dobrychevskii, V. N. Prusakov, A. V. Ryzhkov, S. S. Koroshev, *Dokl. Akad. Nauk SSSR* **1976**, *229*, 641; b) A. A. Artyukhov, S. S. Khoroshev, *Koord. Khim.* **1977**, *3*, 1478.

[8] a) R. Minkwitz, A. Werner, *J. Fluorine Chem.* **1988**, *39*, 141; b) R. Minkwitz, G. Nowicki, *Angew. Chem.* **1990**, *102*, 692; *Angew. Chem. Int. Ed. Engl.* **1990**, *29*, 688; c) R. Minkwitz, G. Nowicki, *Inorg. Chem.* **1991**, *30*, 4426; d) R. Minkwitz, G. Nowicki, *Inorg. Chem.* **1992**, *31*, 225; e) R. Minkwitz, G. Nowicki, B. Bäck, W. Sawodny, *Inorg. Chem.* **1993**, *32*, 787, and references therein.

[9] F. Grandinetti, F. Pepi, A. Ricci, *Chem. Eur. J.* **1996**, *2*, 495, and references therein.

[10] R. Cipollini, M. E. Crestoni, S. Fornarini, *J. Am. Chem. Soc.* **1997**, *119*, 9499, and references therein.

[11] a) A. Fiedler, D. Schröder, W. Zummack, H. Schwarz, *Inorg. Chim. Acta* **1997**, *259*, 227; b) G. A. Janaway, M. Zhong, G. G. Gatev, M. L. Chabinyc, J. Brauman, *J. Am. Chem. Soc.* **1998**, *48*, 11697; c) J. Hu, B. T. Hill, R. R. Squires, *J. Am. Chem. Soc.* **1998**, *48*, 11699; d) M. Aschi, J. N. Harvey, C. Schalley, D. Schröder, H. Schwarz, *J. Chem. Soc. Chem. Commun.* **1998**, 531.

[12] a) D. R. Yarkony in *Atomic, Molecular and Optical Physics Handbook* (Ed.: W. F. Drake, ■■ Gordon), AIP Press, Woodbury, New York, **1996**, p. 357, and references therein; b) E. E. Nikitin in ref. [12a], p. 561, and references therein; c) J. C. Lorquet in *The Structure, Energetics and Dynamics of Organic Ions* (Eds.: T. Baer, C. Y. Ng, I. Powis), Wiley, New York, **1996**; d) H. Nakamura, *Annu. Rev. Phys. Chem.* **1997**, *48*, 299; e) S. Shaik, M. Filatov, D. Schröder, H. Schwarz, *Chem. Eur. J.* **1998**, *4*, 193, and references therein; f) J. E. Stevens, Q. Cui, K. Morokuma, *J. Chem. Phys.* **1998**, *108*, 1544.

[13] a) F. Grandinetti, J. Hrusàk, D. Schröder, S. Karrass, H. Schwarz, *J. Am. Chem. Soc.* **1992**, *114*, 2806; b) F. Cacace, F. Grandinetti, F. Pepi, *Angew. Chem.* **1994**, *106*, 104; *Angew. Chem. Int. Ed. Engl.* **1994**, *33*, 123; c) M. Aschi, F. Grandinetti, F. Pepi, *Int. J. Mass Spectrom. Ion Processes* **1994**, *130*, 117; d) M. Aschi, F. Cacace, F. Grandinetti, F. Pepi, *J. Phys. Chem.* **1994**, *98*, 2713; e) F. Cacace, F. Grandinetti, F. Pepi, *J. Phys. Chem.* **1994**, *98*, 8009; f) F. Cacace, F. Grandinetti, F. Pepi, *J. Chem. Soc. Chem. Commun.* **1994**, 2173; g) F. Cacace, F. Grandinetti, F. Pepi, *Inorg. Chem.* **1995**, *34*, 1325; h) F. Grandinetti, P. Cecchi, V. Vinciguerra, *Chem. Phys. Lett.* **1997**, *281*, 431.

[14] *FT-ICR/MS: Analytical Applications of Fourier Transform Ion Cyclotron Resonance Mass Spectrometry* (Ed.: B. Asamoto), VCH, Weinheim, **1991**.

[15] a) R. M. Reese, V. H. Dibeler, *J. Chem. Phys.* **1956**, *24*, 1175; b) V. Tarnovsky, A. Levin, K. Becker, R. Basner, M. Schmidt, *Int. J. Mass Spectrom. Ion Processes* **1994**, *133*, 175.

[16] T. Su, M. T. Bowers, *Int. J. Mass Spectrom. Ion Phys.* **1973**, *12*, 347.

[17] Unless stated otherwise, all experimental thermochemical data are taken from S. G. Lias, J. A. Bartmess, J. F. Liebman, J. L. Holmes, R. D. Levin, W. G. Mallard, *J. Phys. Chem. Ref. Data* **1988**, *17*, Suppl. 1.

[18] L. A. Curtiss, K. Raghavachari, G. W. Trucks, J. A. Pople, *J. Chem. Phys.* **1991**, *94*, 7221.

[19] a) R. D. J. Froese, S. Humbel, M. Svensson, K. Morokuma, *J. Phys. Chem.* **1997**, *101*, 227; b) A. M. Mebel, K. Morokuma, M. C. Lin, *J. Chem. Phys.* **1995**, *103*, 7414.

[20] a) J. F. Harrison, C. W. Eakers, *J. Am. Chem. Soc.* **1973**, *95*, 3467; b) Z.-L. Cai, *Chem. Phys. Lett.* **1993**, *202*, 70.

[21] a) A. B. Cornford, D. C. Frost, F. G. Herring, C. A. McDowell, *J. Chem. Phys.* **1971**, *54*, 1872; b) A. B. Cornford, D. C. Frost, F. G. Herring, C. A. McDowell, *J. Chem. Soc. Faraday Discuss.* **1972**, *54*, 56.

[22] T. J. Buckley, R. D. Johnson III, R. E. Huie, Z. Zhang, S. C. Kuo, R. B. Klemm, *J. Phys. Chem.* **1995**, *99*, 4879.

[23] S. S. Xantheas, T. H. Dunning, Jr., A. Mavridis, *J. Chem. Phys.* **1997**, *106*, 3280, and references therein.

[24] M. Bettendorff, S. D. Peyerimhoff, *Chem. Phys.* **1985**, *99*, 55.

[25] R. P. Morgan, J. H. Beynon, R. H. Bateman, B. N. Green, *Int. J. Mass Spectrom. Ion Processes* **1978**, *28*, 171.

[26] a) *Collision Spectroscopy* (Ed.: R. G. Cooks), Plenum, New York, **1978**; b) K. Levsen, H. Schwarz, *Angew. Chem.* **1976**, *88*, 589; *Angew. Chem. Int. Ed. Engl.* **1976**, *15*, 509; c) K. Levsen, H. Schwarz, *Mass Spectrom. Rev.* **1985**, *3*, 77; d) J. Bordas-Nagy, K. R. Jennings, *Int. J. Mass Spectrom. Ion Processes* **1990**, *100*, 105.

[27] R. G. Cooks, J. H. Beynon, R. M. Caprioli, G. R. Lester, *Metastable Ions*, Elsevier, Amsterdam, **1973**.

[28] a) J. L. Holmes, J. K. Terlow, *Org. Mass Spectrom.* **1980**, *15*, 393; b) J. L. Holmes, *Org. Mass Spectrom.* **1985**, *20*, 1669; c) R. D. Bowen, D. H. Williams, H. Schwarz, *Angew. Chem.* **1979**, *91*, 484; *Angew. Chem. Int. Ed. Engl.* **1979**, *18*, 451.

[29] We assume that the uncertainty in the entropy term is negligible with respect to the enthalpy term.

[30] a) A. M. Ferrari, P. Ugliengo, E. Garrone, *J. Chem. Phys.* **1996**, *105*, 4129; b) A. J. Lupinetti, S. Fau, G. Frenking, S. H. Strauss, *J. Phys. Chem. A* **1997**, *101*, 9551.

[31] All the sationary points with connectivity similar to **4S** located on the triplet B3LYP/6-31G(d) PES proved to be second-order saddle points, even when the larger 6-311 + G(d) basis set was used.

[32] a) J. I. Brauman, C. A. Lieder, M. J. White, *J. Am. Chem. Soc.* **1973**, *95*, 927; b) W. E. Farneth, J. I. Brauman, *J. Am. Chem. Soc.* **1976**, *98*, 7891; c) W. N. Olmstead, J. I. Brauman, *J. Am. Chem. Soc.* **1977**, *99*, 4219; d) O. I. Asubiojo, J. I. Brauman, *J. Am. Chem. Soc.* **1979**, *101*, 3715.

[33] S. Glasstone, K. J. Laidler, H. Eyring, *The Theory of Rate Processes*, McGraw-Hill, New York, **1941**.

[34] See, for example, a) D. R. Yarkony, *J. Phys. Chem.* **1993**, *97*, 4407; b) M. J. Bearpark, M. A. Robb, H. B. Schlegel, *Chem. Phys. Lett.* **1994**, *223*, 269; c) C. Quiang, K. Morokuma, *Chem. Phys. Lett.* **1996**, *263*, 54.

[35] J. N. Harvey, M. Aschi, H. Schwarz, W. Koch, *Theor. Chem. Acc.* **1998**, in press.

[36] The absolute energies and corrections for the evaluation of the G2MS energies of **TSS** are as follows (in Hartree): CCSD(T)/6-31G(d) =

−366.30769, Δ(MP2) = −0.37661, HLC = −0.08358, ZPE = 0.01561, G2MS (0 K) = −366.75227, G2MS (298.15 K) = −366.74805.

[37] B. A. Rumpf, P. J. Derrick, *Int. J. Mass Spectrom. Ion Processes* **1988**, *82*, 239.

[38] a) M. G. Barlow, R. N. Haszeldine, C. J. Peck, *J. Chem. Soc. Chem. Commun.* **1980**, *158*; b) M. Charpentier, J. Fossey, T. T. Tidwell, S. Wolfe, *Can. J. Chem.* **1987**, *65*, 473; c) N. E. Takenaka, R. Hamlin, D. M. Lemal, *J. Am. Chem. Soc.* **1990**, *112*, 6715; d) M. McAllister, T. T. Tidwell, M. R. Peterson, I. G. Csizmadia, *J. Org. Chem.* **1991**, *56*, 575; e) S. Tajima, S. Tobita, M. Mitani, K. Akuzawa, H. Sawada, M. Nakayama, *Org. Mass Spectrom.* **1991**, *26*, 1023.

[39] a) B. Ciommer, H. Schwarz, *Z. Naturforsch. B* **1983**, *38*, 635; b) T. A. Shaler, T. H. Morton, *J. Am. Chem. Soc.* **1989**, *111*, 6868.

[40] Gaussian 94, Revision E.1, M. J. Frisch, G. W. Trucks, H. B. Schlegel, P. M. W. Gill, B. G. Johnson, M. A. Robb, J. R. Cheeseman, T. A. Keith, G. A. Petersson, J. A. Montgomery, K. Raghavachari, M. A. Al-Laham, V. G. Zakrzewski, J. V. Ortiz, J. B. Foresman, J. Cioslowski, B. B. Stefanov, A. Nanayakkara, M. Challacombe, C. Y. Peng, P. Y. Ayala, W. Chen, M. W. Wong, J. L. Andres, E. S. Replogle, R. Gomperts, R. L. Martin, D. J. Fox, J. S. Binkley, D. J. Defrees, J. Baker, J. P. Stewart, M. Head-Gordon, C. Gonzalez, J. A. Pople, Gaussian, Pittsburgh PA, **1995**.

[41] a) A. D. Becke, *J. Chem. Phys.* **1993**, *98*, 5648; b) P. J. Stephens, F. J. Devlin, C. F. Chabalowski, M. J. Frisch, *J. Phys. Chem.* **1994**, *98*, 11623; c) C. Lee, W. Yang, R. G. Parr, *Phys. Rev. B* **1988**, *37*, 785.

[42] a) R. Ditchfield, W. J. Hehre, J. A. Pople, *J. Chem. Phys.* **1971**, 54, 724; b) W. J. Hehre, R. Ditchfield, J. A. Pople, *J. Chem. Phys.* **1972**, *56*, 2257; c) P. C. Hariharan, J. A. Pople, *Mol. Phys.* **1974**, *27*, 209; d) M. S. Gordon, *Chem. Phys. Lett.* **1980**, *76*, 163; e) P. C. Hariharan, J. A. Pople, *Theor. Chim. Acta* **1973**, *28*, 213.

[43] K. Raghavachari, G. W. Trucks, J. A. Pople, M. Head-Gordon, *Chem. Phys. Lett.* **1989**, *157*, 479.

[44] C. Møller, M. S. Plesset, *Phys. Rev.* **1934**, *46*, 618.

[45] a) R. Krishnan, J. S. Binkley, R. Seeger, J. A. Pople, *J. Chem. Phys.* **1980**, *72*, 650; b) T. Clark, J. Chandrasekhar, G. W. Spitznagel, P. von R. Schleyer, *J. Comput. Chem.* **1983**, *4*, 294; b) M. J. Frish, J. A. Pople, J. S. Binkley, *J. Chem. Phys.* **1984**, *80*, 3265.

[46] D. McQuarrie, *Statistical Mechanics*, Harper and Row, New York, **1976**.

[47] H. B. Schlegel in *Modern Electronic Structure Theory* (Ed.: D. R. Yarkony), World Scientific, Singapore, **1995**, p. 459.

[48] N. Koga, K. Morokuma, *Chem. Phys. Lett.* **1985**, *119*, 371.

[49] W. H. Miller, N. C. Handy, J. E. Adams, *J. Chem. Phys.* **1980**, *72*, 99.

[50] T. H. Dunning, *J. Chem. Phys.* **1971**, *55*, 716.

[51] S. Koseki, M. S. Gordon, M. W. Schmidt, N. Matsunaga, *J. Phys. Chem.* **1995**, *99*, 12764.

[52] S. Koseki, M. W. Schmidt, M. S. Gordon, *J. Phys. Chem.* **1992**, *96*, 10768.

[53] M. W. Schmidt, K. K. Baldridge, J. A. Boatz, S. T. Elbert, M. S. Gordon, J. H. Jensen, S. Koseki, N. Matsunaga, K. A. Nguyen, S. J. Su, T. L. Windus, M. Dupuis, J. A. Montgomery, *J. Comput. Chem.* **1993**, *14*, 1347.

0947-6539/98/0411-2374 $ 17.50+.50/0